Eur. Phys. J. Appl. Phys. **45**, 20301 (2009)
DOI: 10.1051/epjap/2009003

THE EUROPEAN PHYSICAL JOURNAL APPLIED PHYSICS

Theoretical and experimental operating wavelength of GaAs/$Al_{0.25}Ga_{0.75}As$ IR photodetectors

A. Almaggoussi[1,a], A. Abounadi[1], H. Akabli[1], K. Zekentes[2], and M. Androulaki[2]

[1] Équipe d'Étude des Matériaux Optoélectroniques (E.E.M.O.), LP2M2E F.S.T.G., BP 549 Marrakech, Morocco
[2] Foundation for Research and Technology – Hellas (FORTH)/I.E.S.L Microelectronics, Research Group Vassilika Vouton, P.O. Box 1527, 71110 Heraklion, Crete, Greece

Received: 27 October 2008 / Accepted: 9 November 2008
Published online: 31 January 2009 –

Abstract. IR photodetectors based on GaAs/$Al_{0.25}Ga_{0.75}As$ multiquantum wells (QWIP) grown by molecular beam epitaxy (MBE) are studied. The envelop function formalism is used to determine the theoretical intersubband transition energies. The electronic states are calculated in both parabolic and non parabolic cases. IR spectroscopy transmission is used as the experimental technique to evaluate the optical absorption. The measures are made at 77 K for incidence at both 45° and Brewster angles geometries. The last experimental results compare well with the theoretical ones and correspond to 10–12 μm operating wavelength.

PACS. 78.67.De Quantum wells

1 Introduction

The QWIPs are cooled quantum detectors well adapted to military, medical and imaging applications [1–3]. These low dimension hetero-systems has been developed more over the last ten years and now reaches an high level of maturity [4–7]. The IR detection in the GaAs/AlGaAs structure is governed by intersubband transitions in the conduction band. The wavelength spectral response is adjusted while varying both the Al composition and the well thickness.

In Section 2 we give the growth parameters of the studied samples. In Section 3 we give a brief description of the theoretical approach used for the electronic states and energy transition calculations. In Section 4 we present the optical absorption measurements and related modeling.

2 Sample parameters

Two samples were grown using MBE technique. Sample (A) is constituted by 50 periods while sample (B) contains only 8 periods. The structures were grown on GaAs (100) semi-insulating substrate. The growth temperature was kept between 560 and 600 °C. The Al composition was fixed to 25% in both samples while the well thickness was varied. The thickness was determined by X-ray diffraction and confirmed by transmission electron microscopy (TEM) probes. The wells were Silicon doped using δ-doping method. The corresponding parameters are reported in Table 1.

3 Operating wavelength calculations

The electron motion in the envelop function approximation is described by the following Schrodinger equation:

$$\left[-\frac{\hbar^2}{2m^*}\frac{\partial^2}{\partial z^2}+V(z)\right]\chi_n(z)=E_n\chi_n(z) \qquad (1)$$

where E_n and $\chi_n(z)$are respectively the eigenenergy and envelop eigenfunction of the nth subband. $V(z)$ is the conduction band offset. The limit conditions of the wavefunction and its mass pondered derivative specific to superlattices lead to the dispersion equation [8–10]:

$$\cos(qd)=\cos(k_wL_w)\cos(k_bL_b)-\frac{1}{2}\left(-\xi+\frac{1}{\xi}\right)\times\sin(k_wL_w)\sin(k_bL_b)=F(E). \qquad (2)$$

The calculations were made in both parabolic and non-parabolic cases. Nonparabolicity effects have been introduced following Nelson's approach [11] where the energy-dependent effective masses are given by:

$$m_w^*(E)=m_w^*\,(1+E/E_w)\ \text{and}\ m_b^*(E)=m_b^*\left[1-\frac{(V_b-E)}{E_b}\right] \qquad (3)$$

[a] e-mail: almaggoussi@menara.ma

Table 1. Structural parameters of studied samples.

Samples	Structure	Well		Barrier	Number of
		Doping (cm^{-2})	Thickness (Å)	thickness (Å)	periods
A	$Al_{0.25}Ga_{0.75}As$	4×10^{11}	40	500	50
B	$Al_{0.25}Ga_{0.75}As$	5.5×10^{11}	50	500	8

Table 2. Calculated energy levels and wavelength of corresponding transitions.

Sample	x (%)	L_w(Å)	L_b(Å)	E_0 (mev)		E_1 (mev)		λ (μm)	
				Parab	N. parab	Parab	N. parab	Parab	N. parab
A	25	50	500	68.2	66.5	191.22	190.52	10.14	10
B	25	40	500	85	82.8	191.62	191.52	11.63	11.4

where E_w and E_b are the effective energy gaps between the conduction and light-hole valence band respectively in the well and barrier.

Only one level was found to be confined in the well. The transitions are then bound to continuum. The results are reported in Table 2 where E_1 is the first quasi-level located in the continuum.

For both samples the nonparabolicity effect implies a reduction of the confinement energy. This is an expected result when considering usual boundary conditions [12]. The shift of ground state is more important in sample B since it goes higher up in the conduction band.

However, the nonparabolicity effect is small on the E_1 quasi-level. We believe this results from the continuum character of this level.

In all cases and for the two samples the operating wavelength is situated in the long wavelength infrared domain.

4 Absorption measurements

The intersubband transitions in QWIPs are governed by selection rules that appear in the absorption coefficient given by [8,13]:

$$\alpha_p(\omega) = \frac{\pi e^2 \cos^2\theta}{nc\varepsilon_0} \sum \frac{\omega_{if}^2}{\omega} \mu_{if}^2 \left[f(E_f) - f(E_i)\right] \times \frac{\hbar\Gamma}{(E_f - E_i - \hbar\omega)^2 + (\hbar\Gamma)^2}. \quad (4)$$

Only the transverse magnetic (TM) polarization of electromagnetic wave leads to intense interssuband transitions because the strong coupling of light and carriers. Then, the design of QWIPs is mainly based on this consideration. Two major ways are used to maximise the absorption [14–16]. The first one is based on simple pass of light (Figs. 1a and 1b), while the second is based on multipass of light using wave guide technique (Fig. 1c).

In our case, we have used the simple pass technique in two geometrical configurations of light coupling: incidence normally to the 45° polished face (Fig. 1a) and incidence at the Brewster angle (Fig. 1b).

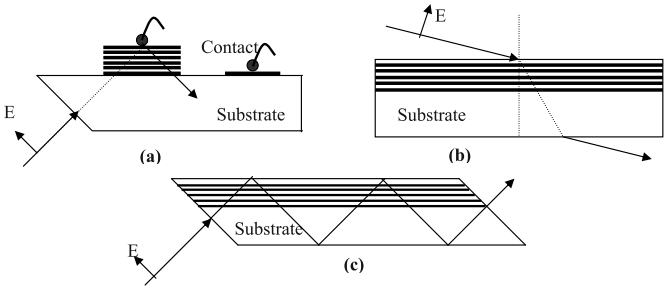

Fig. 1. Light coupling geometries: (a) 45° polissed face; (b) Brewster angle; (c) wave guide multipass.

The total absorption depends also on the refraction angle r and the absorbance is given by:

$$A = N\alpha_p \frac{\sin^2 r}{\cos r}, \quad (5)$$

N is the number of wells in the structure and α_p is the absorption related to one well.

The absorbance is deduced from the transmission measurements following the relation:

$$Absorbance = \log_{10}(T) \quad (6)$$

where T is the transmission of the detector related to the absorption coefficient and its geometry by:

$$T(1-R)^2 e^{-\alpha L} \cong e^{-\alpha N L_P} \quad (7)$$

where $L_P = L_w + L_b$.

FTIR spectrometer was used for measurements. Glow-Bar black-body covering the whole mid-infrared spectrum was used as a source of radiation. Measurements were made at 77 K for both cited geometries.

Figures 2 and 3 show an example of interssuband absorption spectra for both samples. Bold curve represents experimental results while the fine curve represents the Lorentzian modeling corresponding to equation (4).

The obtained spectra are broad and of weak intensity. This is a manifestation of the bound to continuum character of these transitions. The full width at half maximum (FWHM) of the peaks are about 25 meV for both samples leading to relaxation time value of about 0.08 ps. This is

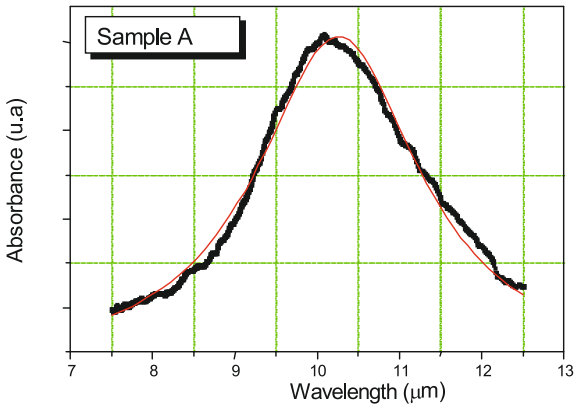

Fig. 2. (Color online) 77 K absorption spectrum of sample A. Bold curve: experiment; fine curve: modeling.

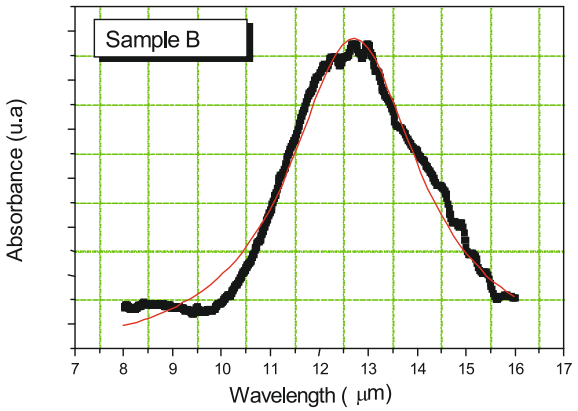

Fig. 3. (Color online) 77 K absorption spectrum of sample B. Bold curve: experiment; fine curve: modeling.

Table 3. Measured operating wavelength.

	Brewster Incidence
Sample	$\lambda_p(\mu m)$
A	10.24
B	12.5
	Incidence at 45°
A	10.2

a small value comparing to the one corresponding to bound to bound transitions [17]. This is probably due to the fact that the corresponding oscillator strength is distributed over the extended states of the continuum.

The operating wavelengths obtained from these spectra are reported in Table 3. Quite good agreement is found between the measured and calculated values.

5 Conclusion

We have grown IR photodetector based on GaAs/AlGaAs multiquantum well by MBE. The measured operating wavelengths lay in the third atmospheric windows (8–12 μm). They were found to agree well with the calculated ones determined upon the envelop function framework and to be reduced by the nonparabolicity effect.

A small relaxation time value was obtained in concordance with bound-continuum transitions.

References

1. M. Hostut, Physica E **39**, 50 (2007)
2. E. Costard, P. Bois, A. De Rossi, A. Nedelcu, O. Cocle, F.H. Gauthier, F. Audier, C. R. Physique **4**, 1089 (2003)
3. D.Z.-Y. Ting, Y.-C. Chang, S.V. Bandara, C.J. Hill, S.D. Gunapala, Infrared Phys. Technol. **50**, 136 (2007)
4. F. Durante, P. Alves, G. Karunasiri, N. Hanson, M. Byloos, H.C. Liu, A. Bezinger, M. Buchanan, Infrared Phys. Technol. **50**, 182 (2007)
5. M. Jhabvala, Infrared Phys. Technol. **42**, 363 (2001)
6. B.F. Levine, J. Appl. Phys. **74**, R1 (1993)
7. M.O. Manasreh, G.J. Brown, *Semiconductor Quantum Wells and Superlattices for Long-Wavelength Infrared Detectors*, edited by M.O. Manasreh (Artech House, Boston, London, 1993), pp. 1–17
8. G. Bastard, *Wave mechanics applied to semiconductor heterostructures* (EDP Sciences, Paris, 1988)
9. C. Liu, D.D. Coon, O. Byungsung, Y.F. Lin, M.H. Francombe, Superlatt. Microstruct. **4**, 343 (1988)
10. G. Bastard, Phys. Rev. B **24**, 5693 (1981)
11. D.F. Nelson, R.C. Miller, D.A. Kleinman, Phys. Rev. B **35**, 7770 (1987)
12. U. Ekenberg, Phys. Rev. B **40**, 7714 (1989)
13. H.C. Liu, *The basic physics of photoconductive quantum well infrared detectors, in Long Wavelength Infrared Detectors*, edited by M. Razeghi (Gordon and Breach Science Publishers, 1996), ISBN 2-88449-208-9
14. M.G. Moharam, D.A. Pommet, E.B. Grann, T.K. Gaylord, J. Opt. Soc. Am. A **12**, 1068 (1995)
15. M.G. Moharam, D.A. Pommet, E.B. Grann, T.K. Gaylord, J. Opt. Soc. Am. A **12**, 1077 (1995)
16. C.J. Chen, K.K. Choi, M. Tidrow, D.C. Tsui, Appl. Phys. Lett. **68**, 1446 (1996)
17. B.F. Levine, A. Zussman, S.D. Gunapala, M.T. Asom, J.M. Kuo, W.S. Hobson, J. Appl. Phys. **72**, 4429 (1992)